Pore-Structure Optimization of Calcium Carbonate for Enhanced Sulfation

Suhas K. Mahuli, Rajeev Agnihotri, Shriniwas Chauk, Abhijit Ghosh-Dastidar, S.-H. Wei, and Liang-Shih Fan
Dept. of Chemical Engineering, The Ohio State University, Columbus, OH 43210

A modified $CaCO_3$ sorbent with an open internal pore structure is prepared and its sulfation characteristics are investigated in an entrained flow reactor at high temperatures (900–1,100°C) and short contact times (20–600 ms) using small particle sizes (< 5 μm). The most distinguishing feature of this modified carbonate (MC) is its 70–75% sulfation conversion within 0.5 s, which is substantially higher than any other sorbents published. The MC is prepared by carbonation-precipitation from a calcium hydroxide suspension by optimizing the operating parameters to generate carbonate particles of the desired pore structural properties. The high initial surface area combined with its open pore structure and pore-size distribution of its calcine contribute to its high reactivity. The calcined MC possesses a significant portion of its pore volume in the 50–200 Å range. This size range represents an optimum pore size for sulfation since it provides a reasonably high surface area and is less susceptible than < 50 Å pore sizes, to pore filling, or pore-mouth plugging due to the formation of higher molar volume $CaSO_4$. Investigation with other carbonates reveals that a much higher portion of their calcines' porosity lies in the smaller pores, which leads to premature termination of sulfation. Results show the impact of internal pore structure on initial reactivity and ultimate sorbent conversion.

Introduction

Calcium-based sorbent powders ($CaCO_3$ or $Ca(OH)_2$) used in the high-temperature removal of SO_2 from combustion systems suffer from rapid loss of reactivity and incomplete utilization. The calcium conversion reaches a maximum of only about 30–35% under the high-temperature conditions (850–1,100°C) of the combustor. Even though promoting these pure sorbents with chemical or structural modifiers has resulted in improved sulfur capture, only a maximum of about 75% sulfur removal (at Ca/S molar ratio of ~ 2) has been achieved with such modified sorbents in the laboratory studies, which falls much shorter of the 90–95% removal goal (Ghosh-Dastidar et al., 1996).

The SO_2 removal process takes place through two reaction steps: calcination (decomposition) of the sorbent to produce high surface area and high porosity CaO, and reaction with SO_2 (sulfation) in the presence of O_2 to form the higher molar volume solid product, $CaSO_4$:

$$Ca(OH)_2 \leftrightarrow CaO + H_2O \quad (1)$$

$$CaCO_3 \leftrightarrow CaO + CO_2 \quad (2)$$

$$CaO + SO_2 + \frac{1}{2}O_2 \leftrightarrow CaSO_4. \quad (3)$$

The sintering of CaO is a concomitant deactivation phenomenon that reduces the available surface area and porosity for sulfation reaction. The CaO sintering rate is strongly influenced by the initial sorbent type and the foreign ions or impurities in the solid. The CaO derived from carbonate (*c*-CaO) sinters at a slower rate than hydroxide-derived CaO (*h*-CaO), and the presence of certain foreign (aliovalent) ions accelerates the rate of sintering (Borgwardt, 1989). There are a number of factors, all of which together play a crucial role

Correspondence concerning this article should be addressed to L.-S. Fan.
Present address of A. Ghosh-Dastidar: Union Carbide Corp., P.O. Box 670, Bound Brook, NJ 08805.

in determining the rate of sulfation and the overall conversion of the sorbent. The particle size is a significant parameter since larger sizes impose transport limitations on both calcination and sulfation reactions. For particles smaller than 5 μm, the size ceases to be a determining factor in the overall reactivity (Milne et al., 1990). Equally important is the pore-size distribution of the parent sorbent and of the CaO. Gullett and Bruce (1987) proposed that there exists an optimum pore-size range, between 50 and 200 Å, which provides sufficient surface area for the sulfation reaction, without causing rapid pore filling and pore-mouth plugging, which results in the premature reaction termination in small pores. For large pores, the surface area to pore volume ratio progressively diminishes, and their contribution to overall sulfation rate becomes less significant. Hence, the relative advantage of one sorbent over another may be caused by one or more of these important chemical and structural parameters. An effective sorbent should meet the necessary criteria of slowing sintering rate, small particle size, and a favorable pore-size structure.

In previous laboratory studies, hydroxides have shown consistently higher sulfur capture than carbonates (Milne et al., 1990; Bruce et al., 1989). The commercial limestone powder used in the SO_2 capture is usually nonporous and possesses a very low surface area (less than 3 m^2/g). On the other hand, the typical calcium hydroxide sorbents possess an initial surface area of 12–18 m^2/g. Ghosh-Dastidar et al. (1996) have shown that the *c*-CaO generated by the calcination of limestone possesses high surface area, but its pores lie predominantly in the less than 50 Å range. These pores are very susceptible to pore blockage and plugging, leading to premature termination of sulfation. The *h*-CaO derived from $Ca(OH)_2$ exhibits larger pore sizes; however, it also sinters at a much faster rate than *c*-CaO, leading to rapid loss of surface area and subsequent deactivation (Ghosh-Dastidar et al., 1996). As a result, both calcium-based sorbents exhibit rapid deactivation and incomplete utilization.

Earlier attempts at improving sorbent reactivity focused on either reducing the CaO particle size or modifying the $Ca(OH)_2$ with structural or chemical promoters to increase its surface area. Investigations with promoted hydrates with high surface area did not exhibit much improvement in overall reactivity (Kirchgessner and Jozewicz, 1989). Sadakata et al. (1994) produced CaO of ultrafine (UF) size of diameter < 0.1 μm by employing a laser ablation method. They reported that the reaction rate of UF CaO particles increased by a factor of 10^2–10^3 in comparison with CaO particles of > 1-μm size. This UF size gave rise to high surface area of CaO, which was mainly external surface area. Steciak et al. (1995) reported calcium magnesium acetate (CMA) as an effective sorbent for combined SO_2–NO_x removal. They observed more than 90% SO_2 removal at 950–1,200°C and Ca:S of 2:1. Calcination of CMA produces thin-walled cenospheres of CaO and MgO with porosities of nearly 70% and surface area of 27 m^2/g. The MgO enhances dispersion of the CaO, thereby reducing its sintering and increasing its accessibility.

The preceding discussion suggests that if the calcium carbonate could be modified to a more open initial pore structure, it could yield higher sulfur capture than the hydrate sorbent particles. Ghosh-Dastidar et al. (1996) have demonstrated that a particular high surface-area limestone (Forsby carbonate (FC), 12 m^2/g) exhibited high sorbent conversion of about 50%. They showed that the FC's initial high surface area and associated pore structure translated into an optimum pore-size distribution in its calcine, which, combined with the effect of slower sintering contributed to its remarkable sulfation capacity. Ye et al. (1995) also compared Forsby with another high surface-area carbonate and concluded that the Forsby's high reactivity was due to its surface area and pore volume located in pores > 50 Å.

In this work, calcium carbonate powder with high surface area and pore volume is prepared by carbonation-precipitation of a calcium hydroxide suspension in a slurry bubble-column reactor in the presence of a small amount of surfactant. The operating parameters of the reactor are optimized to generate carbonate particles of desired pore structural properties. The sulfation characteristics of these sorbent particles are compared with a commercial carbonate and the Forsby carbonate. In addition, a modified calcium hydroxide with pore properties similar to the modified carbonate is studied for comparison. The sulfation studies are carried out in a high-temperature, entrained-flow reactor system. Evolution of pore structure and the subsequent reaction effects on surface area, pore volume, and pore-size distribution are examined for reaction times less than 100 ms. These characteristics are used to elucidate the reasons for high reactivity of the modified carbonate.

Experimental

The modified carbonate (MC) is prepared by carbonation precipitation in a Pyrex reactor, 64 mm in diameter and 380 mm high. A sintered glass plate with a pore opening of 25 to 50 μm (ASTM Por C) is used as the gas distributor. Aqueous suspension of calcium hydroxide (Linwood Mining & Materials Co.) is reacted batchwise with pure CO_2 gas introduced from the bottom of the reactor. Dispex N40V, Dispex A40 (Allied Colloids), and Lignosite 100 (Georgia Pacific) are the surfactants used in small concentrations of about 2 wt. % (based on the weight of calcium hydroxide used). The carbonate used in this study is prepared by bubbling 2.25 L/min of CO_2 through a $Ca(OH)_2$ suspension with solids concentration 2.5 wt. %. A bubbling time of 20 min is sufficient for complete conversion of $Ca(OH)_2$ to $CaCO_3$ (Wei et al., 1997; Fan et al., 1997).

The postreaction slurry is filtered by #1 filter paper and dried in a vacuum oven at 75°C for 24 h. Scanning electron microscopy (SEM) and X-ray diffraction (XRD) are used to study the crystal structure and composition. The primary particle-size distributions are measured by Sedigraph 5100 (Micromeritics).

Entrained-flow reactor system

A specially designed high-temperature, entrained-flow reactor (Figure 1) is used to conduct the short-time kinetic experiments. The system consists of a reactor tube assembly within a multizone high-temperature furnace, a powder feeder, water-cooled injection and collection probes with PC-interfaced data-acquisition systems, and a particle separator/classifier (Raghunathan et al., 1992, 1993; Ghosh-Dastidar et al., 1995). The reactor consists of an outer mul-

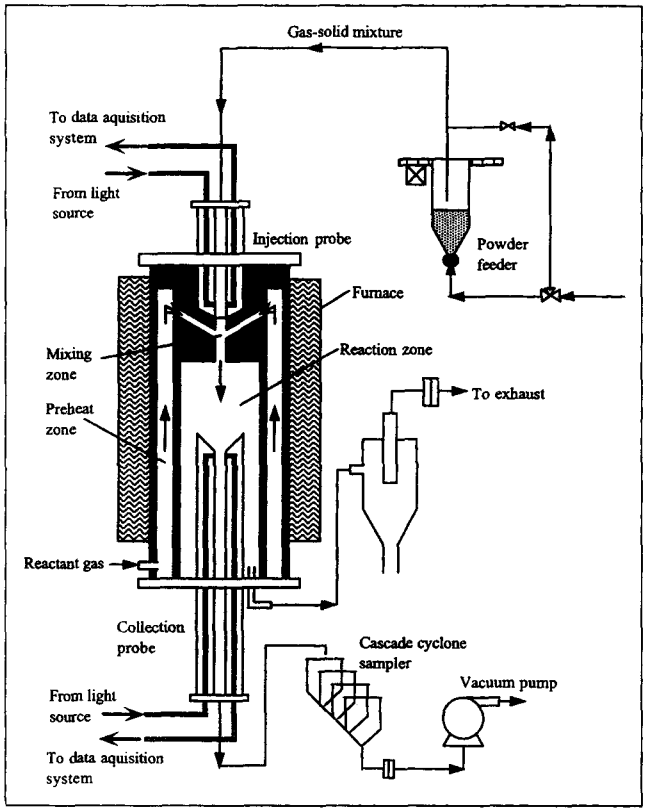

Figure 1. Entrained flow reactor (EFR) system.

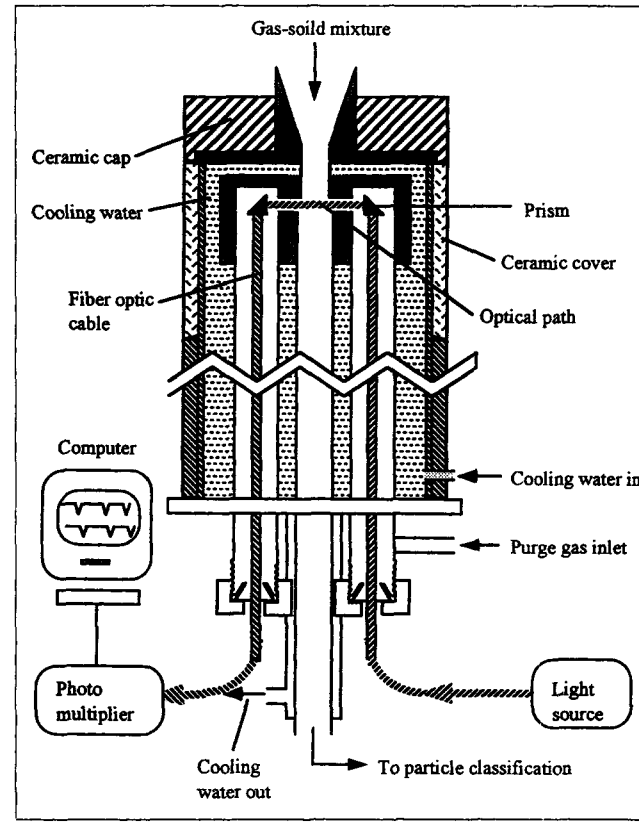

Figure 2. Collection probe.

lite tube and an inner concentric tube assembly, which holds an entrance block between the two tubes. The entrance block is designed for gas entry into the inner tube from the outer annular region and also for instantaneous mixing of injected sorbent and reactant-gas stream. The reactant gas is heated to the desired temperature as it travels up the annular region. After passing through the reaction zone, the sorbent/gas mixture is sampled by the collection probe followed by instant quenching. Positioning the collection probe at different axial locations makes it possible to sample sorbents at various residence times.

The injection probe, located above the entrance block, injects sorbent powder into the incoming hot gas stream. The hot impinging gas stream ensures rapid heating of the solid to the reaction temperature. Both the injection and collection probes house an assembly of two optical guides, which detect any particle flow through the probe tips. For any pulse of solid injected, the combination of probe systems produces two spikes separated by some time interval in the probe signals. The residence time of the sorbent is thus determined on-line from a cross-correlation of these two signals (Raghunathan et al., 1993).

The collection probe is shown in Figure 2. The gas–particle mixture flows through a central hole along the probe axis. Two other identical holes are oriented parallel to the central axis and are used for housing the optical guides. These two holes are connected radially near the probe tip for passage of light, and miniature prisms placed on both sides serve to create a light path. Dry nitrogen is purged through the annular space surrounding the optical guides, which comes in contact with the incoming hot gas–particle mixture, causing rapid cooling. A near-isothermal temperature profile (within ± 10°C of the nominal) is maintained over most of the reaction zone.

The powder is fed continuously at a rate of 300–600 mg/h, ensuring good dispersion of powder and a low solids/gas ratio for differential conditions. The heat-up or quenching rate of particles is estimated for sorbent particles subjected to an increase or decrease in the surrounding temperature and accounting for convection from bulk gas and radiation from reactor wall. The results indicate that the particles that are less than 5 μm in diameter are heated to the final temperature within 2 ms of injection into the hot gas stream. The assumptions involved in the heat-up and quenching calculations, and the detailed heat balance equations are described in Ghosh-Dastidar et al. (1995). Gullett et al. (1988) and Alvfors and Svedberg (1992) also estimated negligible heat-up times for such small particles. Quenching of the reaction is achieved by mixing of the hot particle/gas stream with cold nitrogen purge and by the water-cooling of the collection probe.

Calcination and sulfation studies are performed at a fixed reaction temperature. Calcination is carried out under inert N_2 environment, and the gas composition for the sulfation runs is maintained at 5.45% O_2, 3,900 ppmv SO_2 and balance N_2. The partially reacted sorbents are classified into various size fractions in a cascade cyclone sampler (Andersen Instruments). The sorbents of a particular size group, having a mean aerodynamic diameter of 3.9 μm, are analyzed for determining reaction conversion and performing structural evolution studies. Obtaining these sets of information from

particles of the same size fraction eliminates particle size as a variable parameter between the sorbents.

The FC is received as slurry and is dried and ground, while Linwood carbonate (LC) is used in its as-received form. In order to prepare the modified hydroxide (MH), the as-received Linwood calcium hydroxide powder is calcined at 600°C and then rehydrated in excess water containing dissolved calcium lignosulfonate surfactant. The surfactant is added in such a quantity that the final hydroxide product has 1.5% mass concentration of the lignosulfonate, reported to be optimum by previous investigators (Kirchgessner and Lorrain, 1987).

Conversion and structural analysis

The extent of calcination in the flow reactor is measured by heating a portion of the collected sorbent to its calcination temperature in the TGA and allowing it to decompose to CaO completely. The conversion for sulfation studies is obtained from SO_4^{2-}-ion concentration analysis by Alltech Ion Chromatography (IC) system. The surface area, pore volume, and pore-size distribution of the collected samples are measured by low-temperature nitrogen adsorption in a Quantachrome BET apparatus. In order to include the largest intraparticle pores in the measurement of pore volume, it is necessary to achieve N_2 condensation at a partial pressure close to its saturation pressure. The pore-volume measurement is made at a relative pressure of 0.96, at which the Kelvin equation predicts that pores up to 252 Å in radius are filled. This ensures inclusion of most of the intraparticle pores while omitting the interparticle voids. Another significant point to note is that while the pore sizes of carbonate-calcines are presented in terms of pore radius, those for the hydroxide-calcines are reported as separation between plates. This accounts for the difference in pore shape between carbonate and hydroxide calcines. Gullett and Bruce (1987) suggest that while *c*-CaO possesses cylindrical pores, *h*-CaO can be best represented by a parallel-plate pore structure.

Results and Discussion

Sulfation kinetics of MC

The short-time sulfation kinetics of 3.9 μm (aerodynamic size) MC particles is investigated at three temperatures, 900, 1,000 and 1,080°C for residence times ranging from 20 ms to 600 ms. As seen in Figure 3, the most distinguishing feature of the MC sulfation is its 70–75% conversion, which is much higher than the conversion of any other sorbent reported in the literature under similar particle-size and reaction conditions. MC does exhibit both the characteristics typical of sulfation reaction, namely, the very high initial reaction rate and the severe attenuation at longer contact times. Both 1,000 and 1,080°C show similar conversions achieving nearly 50% conversion in the first 40 ms. At higher residence times, however, there is a considerable reduction in overall reaction rate, especially at 1,080°C, which shows a flat conversion profile, and 1,000°C exhibits higher conversions than 1,080°C beyond 200 ms. At 900°C, the conversion increases initially at a slower rate but the flattening of the conversion profile is not as severe as at the higher temperatures and about 50% conversion is achieved at 600 ms.

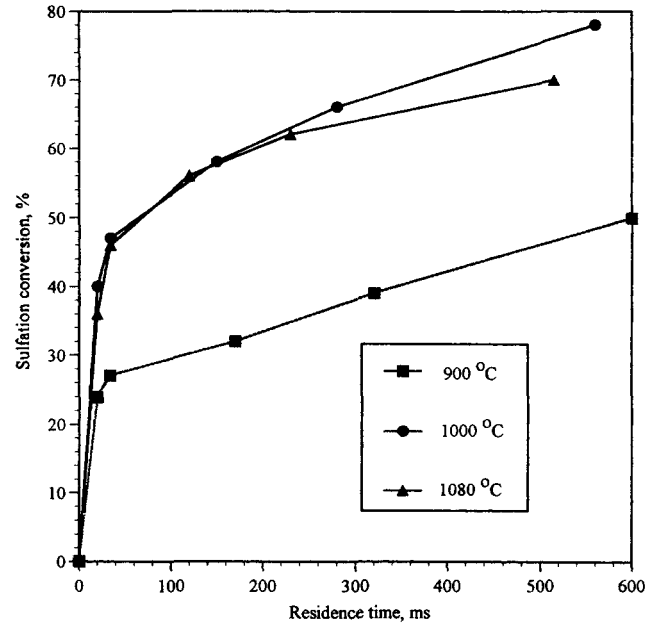

Figure 3. Influence of temperature on sulfation of MC.

For small particles it is generally accepted that the sulfation rate increases with increasing temperature till the equilibrium limitation becomes evident. However, sintering also becomes very significant above 1,000°C, depleting the surface area and pore volume available for the sulfation reaction. These two opposing mechanisms together yield an optimum temperature that exhibits the highest ultimate conversion. As seen in Figure 3, there is a dramatic increase in reactivity between 900 and 1,000°C; evidently the increase in sulfation kinetics compensates for any increase in rate of sintering. In order to investigate the optimum temperature for MC, the extent of conversion after 530 ms of sulfation is analyzed at various temperatures between 900 and 1,115°C for 3.9-μm particles. Figure 4 shows that a maxima in the conversion exists at 1,000°C with a sulfation extent of about 78. This temperature trend compares well with results previously reported in the literature for other carbonate sorbents of similar particle sizes (Ye et al., 1995; Cole et al., 1985).

The sulfation characteristics of MC are compared with three other sorbents—the FC, the LC, and the modified Linwood hydrate—under identical reaction conditions. The chemical composition and the initial surface area and pore volume of all the sorbents are shown in Table 1. The primary particle-size distribution of the sorbents, as shown in Figure 5, illustrates that all the sorbents possess a similar unimodal distribution and their d_{50} lie in the narrow range between 1 and 2 μm, except for LC, which is significantly coarser. As shown in Figure 6, the initial reaction rate of MC is more than two times that of LC, while its ultimate conversion is nearly three times that of the commercial LC. The LC shows a virtual reaction die-off beyond 100 ms, and its long-time conversion values of about 28% match with those reported by previous researchers (Milne et al., 1990; Gullett et al., 1988). The modified hydrate (MH) possesses a surface area and porosity similar to the modified carbonate, and yet shows a final conversion of only about 35%. These conversion data for MH carroborate the findings by Kirchgessner and

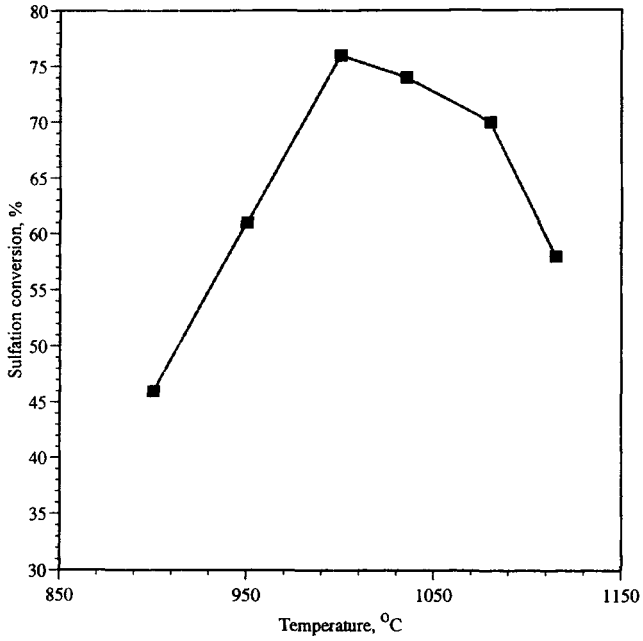

Figure 4. Temperature variation in sulfation of MC.
Residence time: 510 ms; particle size: 3.9 μm.

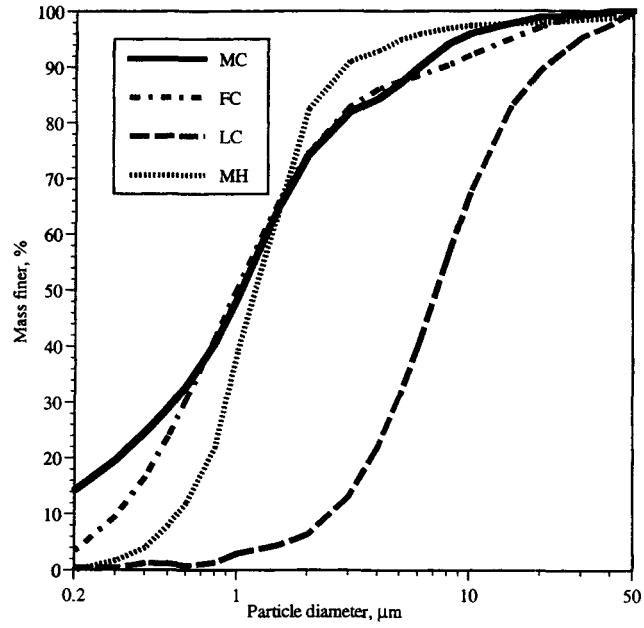

Figure 5. Primary particle-size distribution from sedigraph analysis.

Jozewicz (1989) that addition of lignosulfonate additive results in about 35% final sorbent conversion. The only sorbent that exhibits an initial reaction rate comparable with the MC is the FC. The ultimate conversion exhibited by FC is about 50%, and compares well with the observations of Ye (1994) and Wang et al. (1995).

To confirm that the particle size is small enough to eliminate intraparticle diffusional and heat-transfer limitations, sulfation conversions of various particle sizes at 1,000°C are analyzed, as shown in Figure 7 for MC. The 3.9-μm and 1.7-μm particles do not exhibit any difference in the initial rate or the longer-time conversion. Ghosh-Dastidar et al. (1996) showed that the FC and MH also do not show significant particle-size effect below about 5 μm. A similar observation was made by other investigators (Milne and Pershing, 1987; Cole et al., 1986) studying particle-size effect on sulfation.

Table 1. Chemical Composition and Initial Structural Properties of Sorbents

Composition wt. %	Modified Hydroxide	Linwood Carbonate*	Forsby Carbonate**	Modified Carbonate
$Ca(OH)_2$	93.6	—	—	—
$CaCO_3$	1.0	97.0	95.6	97.0
SiO_2	0.8	0.8	0.26	0.9
Al_2O_3	0.6	0.5	0.30	0.6
MgO	1.0	—	0.88	1.0
CaO	1.0	—	—	—
Fe_2O_3	0.5	0.5	0.23	0.5
$MgCO_3$	—	1.0	—	—
Cal. ligno sulfonate†	1.5	—	—	—
BET Surface area (m^2/g)	62.0	1.9	12.0	61.0
Pore vol. (cm^3/g)	0.115	0.004	0.04	0.121

*Linwood Mining and Minerals Co.
**Carbital Co., Sweden.
†Georgia-Pacific Corp.

Pore-structure development with calcination and sulfation

Since the external diffusional limitations do not play any role in dictating the sulfation characteristics of these small-size particles, the factors influencing the sulfation behavior

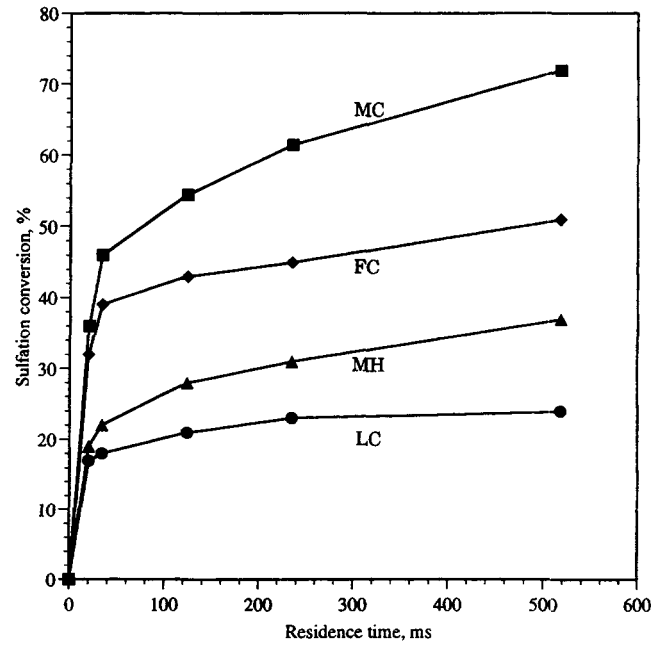

Figure 6. Sulfation of MH, LC, FC and MC.
Reaction temperature: 1,080°C; particle size: 3.9 μm.

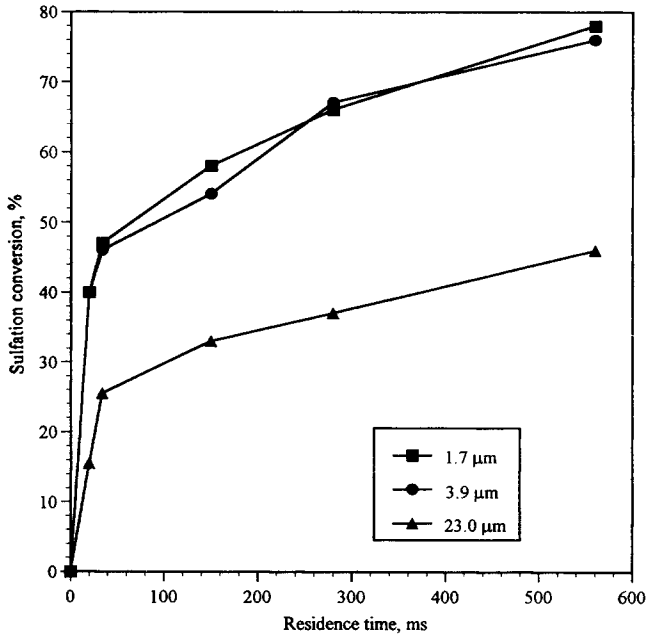

Figure 7. Effect of particle size on sulfation conversion of MC at 1,000°C.

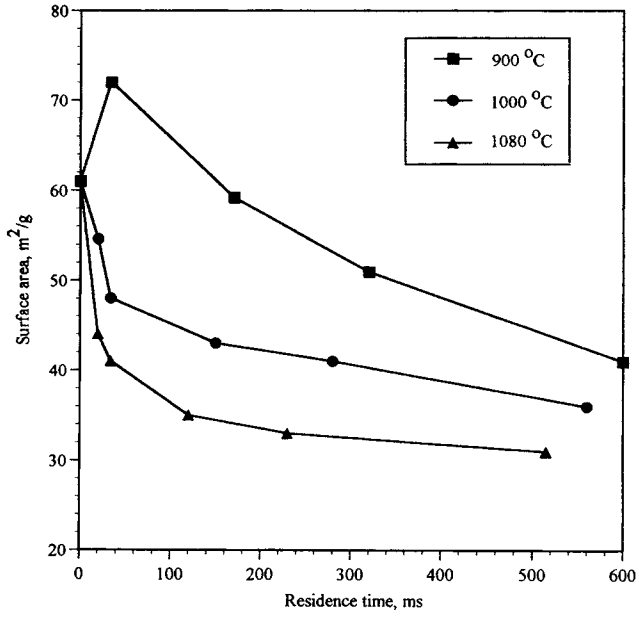

Figure 9. Effect of temperature on surface area evolution during calcination of MC.

Particle size: 3.9 μm.

must be associated with the CaO internal structure, which develops from the decomposition reaction and alters with sintering and sulfation. Of primary interest should be the pore structure data of the first 50 ms, in which the bulk of the sorbent conversion is completed and also the extent of the succeeding reaction rate is determined.

Calcination and Pore Evolution of MC. The calcination kinetics and surface area and pore structure distribution changes are studied for MC in order to gain insights into its high reactivity and the effect of temperature. Figure 8 shows the extents of calcination, and Figure 9 shows the corresponding surface area of the partially calcined MC particles. Calcination of MC also exhibits a very high initial rate of decomposition, and nearly 75% of the ultimate calcination is achieved in the first 50 ms. Almost complete calcination is achieved at 1,080 and 1,000°C, but 900°C exhibits a slower rate of calcination and reaches only about 85% calcination even after 600 ms. The strong influence of sintering is clearly visible at 1,080°C, which shows a very high rate of surface-area loss, even at short contact times. This indicates that the surface-area loss due to sintering more than compensates for the additional surface area being produced by the calcination reaction. The rate of sintering is strongly dependent on the surface area of the sintering CaO and is accepted to follow second-order kinetics as proposed by Nicholson's (1965) model (Ghosh-Dastidar et al., 1995; Mai and Edgar, 1989; Silcox et al., 1989)

$$\frac{dS}{dt} = -k_s(S - S_a)^2, \tag{4}$$

where S is the surface area at time t; S_a is the asymptotic surface area; and k_s is the specific sintering rate constant. Due to the high surface area of the MC itself, the surface area of its nascent calcine can be expected to be very high. As a result, the rate of surface-area reduction is the highest in the initial few milliseconds, when the surface area of the nascent calcine is the greatest. At higher residence times, the surface area approaches the asymptotic value and the rate of sintering is much slower. On the contrary, 900°C shows a maxima in the surface area at about 34 ms in spite of the calcination extent being 76%.

Figure 10 shows the variation of the total pore volume with time. The pore volume is seen to increase for all the three temperatures initially. However, the increase is not commen-

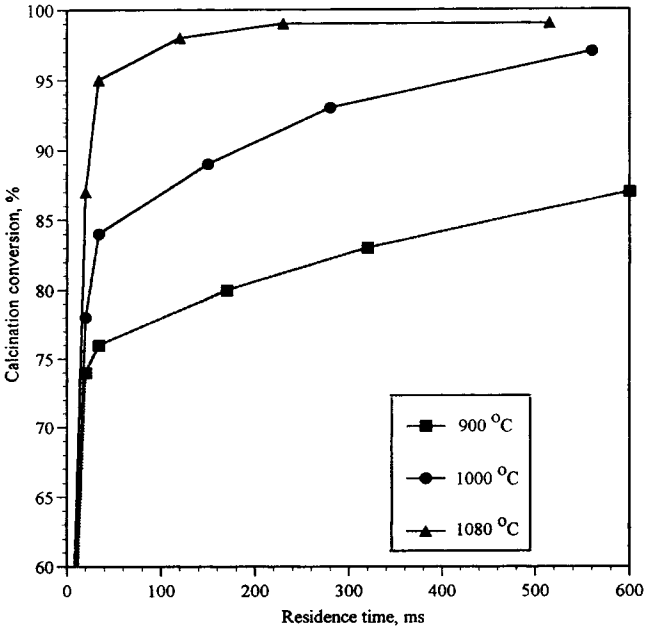

Figure 8. Influence of temperature on calcination of MC.

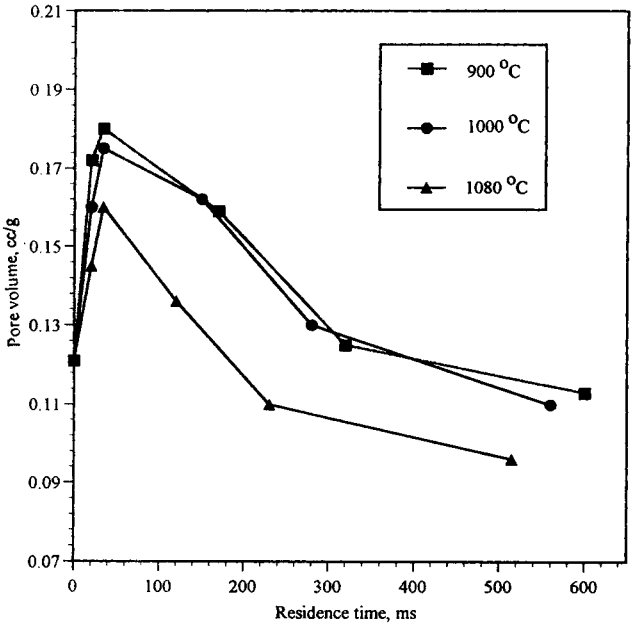

Figure 10. Influence of temperature on pore volume evolution during calcination of MC.

Particle size: 3.9 μm.

surate with the theoretically predicted amount of pore volume based on the molar volume of $CaCO_3$ and CaO. This indicates that sintering does consume a substantial amount of the pore volume also. Moreover, sintering also leads to a disappearance of the small pores that combine to yield larger pores, thus shifting the pore-size distribution to larger sizes. This might give rise to pores larger than 500 Å in diameter. The measurement of such large pore sizes would entail interference with the interparticle voids and moreover, such large pores contribute negligible surface area for the sulfation reaction. The desorption isotherm is used for these calculations, and the Kelvin equation forms the basis for determining the pore-size distribution:

$$r_p - t = \frac{2\gamma V_L}{RT \ln\left(\frac{P_0}{P}\right)}, \tag{5}$$

where r_p indicates the actual radius of the pore in which condensation occurs at the relative pressure, P/P_0, and t is the thickness of the adsorbed film. At the relative N_2 pressure of 0.96, all the pores of sizes up to 252 Å are assumed to be completely filled, and this also corresponds to the total pore volume of the solid. The pore-volume distribution after 20 ms of calcination is similar at all of the three temperatures. This indicates that the primary difference between the three temperatures is due to the surface-area evolution. The 1,000°C shows a similar rate of calcination and a higher surface-area retention compared to 1,080°C, which leads to its comparable rate of sulfation in the initial 50 ms. At longer times, 1,000°C is seen to possess a higher surface area (Figure 9) as well as pore volume (Figure 10) than 1,080°C, which would help in the higher overall sulfation conversion at 1,000°C than at 1,080°C, as seen in Figure 3.

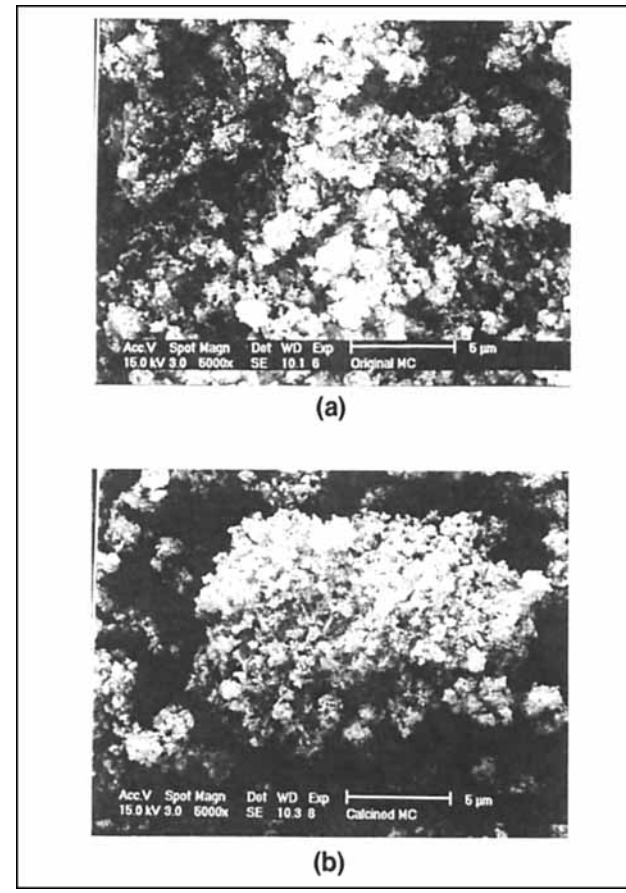

Figure 11. Scanning electron micrographs of MC and MC-calcined at 900°C for 600 ms.

SEM analyses are conducted to complement the studies of structural changes accompanying the simultaneous calcination and sintering. Figure 11 shows the scanning electron micrographs of original MC and MC calcined at 900°C for 600 ms. The calcium-based sorbents undergo size variations due to fragmentation and/or agglomeration in the high-temperature reaction environment. In order to analyze the mechanical strength and fracturability of the MC particles, the effect of high-temperature environment on the particle-size distribution of the MC is studied using Sedigraph analysis of the original MC and of the partially calcined MC following 170 ms of calcination at 1,000°C. Hu and Scaroni (1995) have shown that calcination and subsequent CO_2 pressure buildup within the particles can lead to fragmentation. They studied particle sizes between 37 and 105 μm and found that the dolomitic carbonates were more susceptible to fragmentation than the carbonate particles. However, in the case of small particle sizes (< 10 μm), agglomeration can take place during fluidization in the particle feeder unit and breakup may occur during transport due to the fluid-shear (Ghosh-Dastidar et al., 1994; Lee and Fan, 1993). All these factors together dictate the particle-size distribution and its variations. The particle-size distribution is found to change only slightly from the original to the calcined MC. The CO_2 pressure buildup can be discounted in the case of MC due to its small

particle size and its high porosity, thus leading to lesser fragmentation tendency.

Porosity Changes During Sulfation of MC. The formation of the larger molar volume product $CaSO_4$ leads to loss of pore volume through pore filling or pore-mouth closure. In the case of presintered CaO, the porosity change is due to the sulfation reaction alone and can be obtained from a volume balance (Bhatia and Perlmutter, 1981a):

$$\frac{\epsilon}{\epsilon_0} = 1 - \frac{(z-1)(1-\epsilon_0)X_s}{\epsilon_0}, \tag{6}$$

where ϵ_0 represents the porosity of the calcined and sintered CaO. In our case, the sulfating sorbent is undergoing concomitant porosity changes due to calcination and sintering. The predicted porosity of the sorbent is calculated with the following assumptions. The extent of CaO pore reduction due to sintering is assumed to be identical for both sulfation (with SO_2) and calcination (without SO_2) reactions. The extent of hydroxide or carbonate decomposition to CaO is assumed to be unaffected by the presence of SO_2. The fraction of CaO (w_C) per unit weight of partially calcined product can be expressed as

$$w_C = \frac{X_c}{\frac{M_s}{M_C}(1-X_c)+X_c}, \tag{7}$$

where M_s and M_C are molecular weights of the sorbent and CaO, respectively. During sulfation reaction, a fraction of this w_C converts to $CaSO_4$. If the overall sulfation conversion is expressed as X_s, the amount of $CaSO_4$ can be obtained as

$$W_p = X_s\left(\frac{w_C}{M_C} + \frac{w_s}{M_s}\right)M_p, \tag{8}$$

where M_p is the molecular weight of the product, $CaSO_4$. The amount of residual CaO is

$$W_C = \left[\frac{w_C}{M_C} - X_s\left(\frac{w_C}{M_C} + \frac{w_s}{M_s}\right)\right]M_C. \tag{9}$$

The additional volume occupied by the product $CaSO_4$ is due to its higher molar volume (v_p) compared to that of CaO (v_c). If V_c is the specific pore volume after calcination, then the predicted pore volume after equal duration of sulfation per unit weight of sulfated sample can be expressed as

$$V_{\text{pred}} = \frac{\left[V_c - X_s(v_p - v_c)\left(\frac{w_C}{M_C} + \frac{w_s}{M_s}\right)\right]}{(w_s + W_C + W_p)}. \tag{10}$$

The pore volume values for MC are calculated and plotted in Figure 12 with the experimentally obtained values. The negative values of the predicted pore volumes can be interpreted as higher-than-theoretically predicted sulfation of MC. Gullett and Bruce (1987) investigated sulfation by *h*-CaO and *c*-CaO and attributed the higher-than-theoretically predicted sulfation by *h*-CaO to particle expansion. Their tests with mercury porosimetry indicated expansion in the interparticle region of *h*-CaO, and tests with nitrogen adsorption/desorption indicated that nitrogen is capable of expanding the *h*-CaO and increasing the void space by as much as 25%. They concluded that the formation of $CaSO_4$ must be able to produce even greater expansion than indicated by nitrogen adsorption/desorption, and hence be able to show maximum conversions that indicate about 30% particle expansion. The MC at 520 ms is analyzed to need a particle expansion of nearly 35% to accommodate the higher molar volume product. Another possible factor is the effect of sintering on pore volume is diminished in the presence of SO_2. Newton et al. (1989) performed calcination and sulfation experiments in the presence of CO_2 and observed a reduction in sintering effect during sulfation. They concluded that during sulfation, the influence of CO_2 in accelerating the rate of sintering is inhibited due to the product layer surrounding the CaO grains.

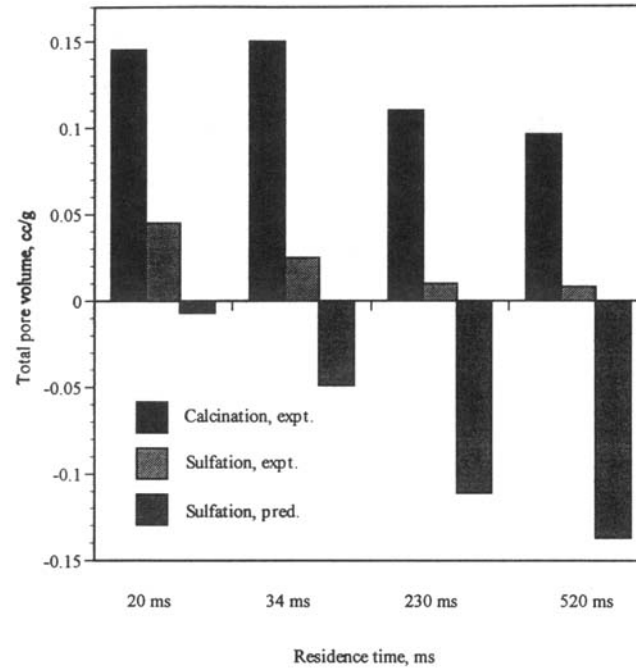

Figure 12. Comparison of experimental pore volume after sulfation at various residence times with that predicted from calcination results.
Reaction temperature: 1,080°C.

Product-layer Diffusion. It is accepted that the solid-state ionic diffusion through the product $CaSO_4$ layer is the controlling mechanism for the sulfation reaction (Bhatia and Perlmutter, 1981b, Sotirchos and Yu, 1985). This is based on the activation energy of diffusion as well as the surface-area dependence (Borgwardt and Bruce, 1987; Borgwardt et al., 1987). The conversion vs. time data is used to evaluate the product-layer diffusivity as follows. Bhatia and Perlmutter (1981a, 1983) formulated the random pore model, which accounts for product-layer expansion due to the larger molar volume of $CaSO_4$ relative to CaO. In the case of product-layer diffusion controlling, the model gives

$$\left\{\frac{1}{\Psi}\left[\sqrt{1-\Psi\ln(1-X_s)}-1\right]\right\}^2 = k_d t, \qquad (11)$$

where,

$$k_d = \frac{M_c D_p C_s S_0^2}{2\rho z(1-\epsilon_0)^2} \qquad (12)$$

and

$$S_0 = \rho(1-\epsilon_0)S_g \qquad (13)$$

$$\Psi = \frac{4\pi L_0(1-\epsilon_0)}{S_0^2}. \qquad (14)$$

The values of the pore-structure parameter Ψ typically vary from 1.2 to 2.5 (Borgwardt et al., 1987). The time required to reach a given conversion decreases with the square of the surface area. The value of k_d is calculated by fitting the X_s vs. t experimental data to the lefthand side of Eq. 11 to minimize the deviation. The D_p value is calculated from Eq. 12 using S_g values from the calcination experimental data (Figure 9) and $M = 56$ g/mol, $C_s = 1.7\times10^{-7}$ mol/cm^3 (3,900 ppm), $\rho = 3.32$ g/cm^3, and $z = 3.09$. Using a value of $\Psi = 1.2$ (Borgwardt et al., 1987) and using only the experimental data beyond the initial 30 ms, it is found that the value of D_p is 30×10^{-12} m^2/s at 1,000°C, which compares well with 69×10^{-12} m^2/s obtained by Bhatia and Perlmutter (1981b) at 980°C. The reported values of activation energy for product-layer diffusion vary from 30 kcal/mol to nearly 40 kcal/mol (Borgwardt et al., 1987). The activation energy is calculated to be 37.5 kcal/mol in this study for product-layer diffusion-controlled sulfation of MC. Borgwardt and Bruce (1986) obtained 36.6 kcal/mol, Bruce et al. (1989) obtained 39 kcal/mol for c-CaO particles, and Hartman and Trnka (1980) obtained 34 kcal/mol for limestone particles. The reported values lie within the range normally seen for diffusion of ions by thermally induced lattice defects (Bruce et al., 1987). The preceding calculations are based on the SO_3^{2-} ions diffusing through the product layer to the $CaO/CaSO_4$ interface. Recently, Hsia et al. (1993, 1995) examined the mechanism of diffusion by conducting inert marker experiments and ^{34}S isotope experiments. They established that the ionic diffusion takes place by the outward diffusion of Ca^{2+} ions and O^{2-} ions in a coupled manner from the $CaO/CaSO_4$ interface to the $CaSO_4$/gas interface. At the $CaSO_4$/gas interface, the sulfation reaction takes place as

$$Ca^{2+} + O^{2-} + \frac{1}{2}O_2 + SO_2 \leftrightarrow CaSO_4. \qquad (15)$$

Comparison with other sorbents

In order to explain the high reactivity of the MC, its pore structural evolution is studied with calcination and sulfation and compared with FC, LC, and MH. Figure 13 shows the initial pore-volume distributions for the sorbents. The modified hydrate and the modified carbonate possess similar pore volume as well as surface area. In addition to the pore-volume distribution, the distribution of surface area in the various

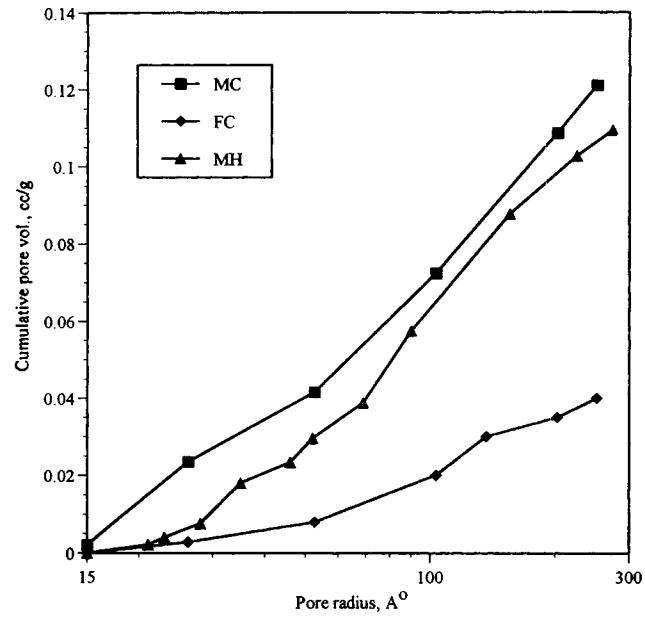

Figure 13. Comparison of pore volume distributions of sorbents before calcination.

pore sizes is investigated for the calcines. The surface-area distribution is theoretically calculated from the pore-size distribution (Gregg and Sing, 1982). The cumulative surface-area value at any pore radius, r, represents the total amount of surface area residing in the pores of radius, r, or larger. The overall surface area of the calcine (A) can be calculated by summation over all size intervals as

$$A = \Sigma\frac{2V_p}{r_p}, \qquad (16)$$

where V_p represents the actual pore volume in each size interval. For the hydrate sorbent, it is accepted that its calcine possesses a parallel-plate-shaped pore structure (Gullett and Bruce, 1987). The pore-volume distribution and the surface-area distribution procedure for the hydrate is similar to the carbonate except the pore radius, r_p, is replaced by the plate width, d, and $(r_p - t)$ is replaced by $(d - 2t)$ in Eqs. 5 and 16 (Innes, 1957).

Figure 14 corresponds to the pore-volume distributions after 34 ms of calcination at 1,080°C, and Figure 15 shows the corresponding surface-area distributions. Calcination conversion data show that for high temperature and small particle size, there is no appreciable difference between the three carbonates and modified hydroxide in CaO generation rate (Ghosh-Dastidar et al., 1996), with all the sorbents exhibiting between 85 and 95% decomposition after 34 ms. Upon comparing the carbonates, the surface area of FC–CaO is greater than MC–CaO, and the LC–CaO also shows a high surface area. Yet the sulfation extents of the carbonates are considerably different from each other, which indicates that the surface area of the calcine alone cannot be used to predict their sulfation behavior.

Only about 35% of total pore volume of LC–calcine lies in pores > 50 Å in size, while the surface-area distribution indi-

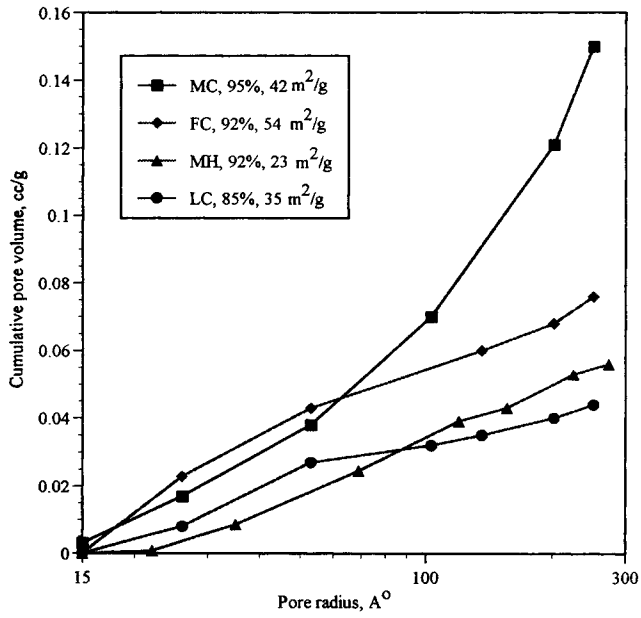

Figure 14. Comparison of pore volume distributions after 34 ms of calcination at 1,080°C.

Particle size: 3.9 μm.

cates only about 10% of surface area in > 50 Å pores for LC. The FC–calcine possesses about 45% of its pore volume and about 15% of its surface area in pore sizes greater than 50 Å. On the contrary, nearly 75% of the MC–calcine pore volume lies in the 50–200-Å size range. This leads to nearly 50% of the surface area in this pore-size range for the MC–calcine.

Upon comparison of the original sorbent pore-volume distributions (Figure 13) and the distribution in their calcines after 34 ms (Figure 14), it can be seen that the FC shows a

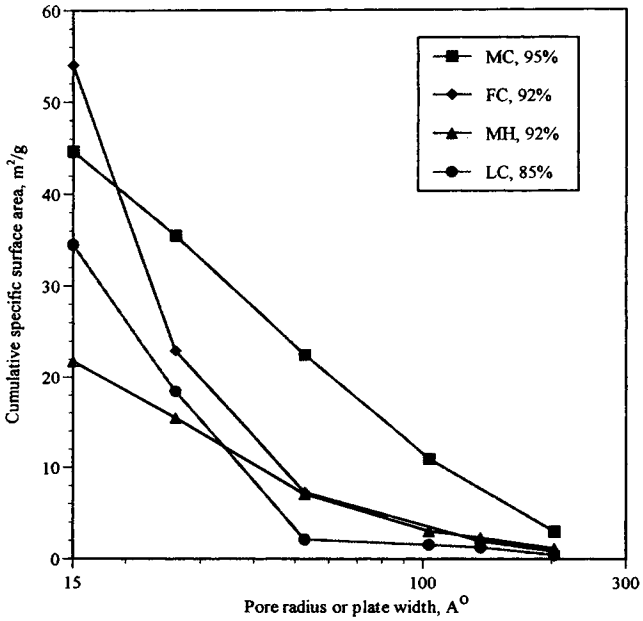

Figure 15. Specific surface-area distribution after 34 ms of calcination at 1,080°C.

Particle size 3.9 μm.

4-times addition to the pore volume in the < 50 Å sizes, while the MC shows that the pore volume in the < 50 Å sizes remains nearly unaltered. The total surface area of the MC–CaO has reduced from 61 m^2/g (original sorbent) to 42 m^2/g, which is lower than the FC–CaO (54 m^2/g). Since the MC-, FC-, and LC–CaO are derived from carbonates of similar chemical composition, and show similar extent of decomposition, a probable explanation for the differences in their pore volume and surface-area distributions can be as follows: the original MC possesses substantial pore volume and surface area in the smaller sizes. The nascent MC–CaO formed in the pores < 50 Å in the initial few milliseconds possesses extremely high surface area, which cannot be sustained and is consumed rapidly by sintering. As a result, the pore-structure data of MC-calcine at 34 ms does not exhibit high surface area. The FC and the LC, on the other hand, do not possess high volumes in the < 50-Å sizes, and upon calcination generate pore volume and surface area that can be sustained. As a result, all the three carbonate calcines possess similar pore volumes in the < 50-Å range, as seen in Figure 14.

In comparison, the MH–CaO has the lowest surface area of all the calcines, and unlike the carbonate calcines its pore volume decreases from the parent sorbent. Both these indicate an extremely high degree of sintering. MH also shows a reduction in the 50–200 Å pores, while all of the three carbonate calcines exhibited an increase. In the case of MH, the high nascent surface area of its calcine combined with the higher sintering of hydrate-derived calcines together lead to the poor pore properties of its calcine. One possible explanation for the lower sintering rate of carbonate-derived calcines, as proposed by Borgwardt (1989), is that due to differences in molar volumes between $CaCO_3$ and $Ca(OH)_2$, packing of CaO grains produced from carbonates is relatively less dense, which offers fewer contact points between these grains. Borgwardt (1989) further reported that even though the activation energies of sintering for hydroxide and carbonate calcines are comparable, the sintering rate constant for the latter is one order of magnitude less than that of the former.

Figures 14 and 15 elucidate two contributing factors that lead to the higher reactivity of MC. First, its calcine provides a high surface area and pore volume. Second, MC–CaO also possesses a favorable pore-size distribution, which distinguishes this sorbent from other carbonates. More than 90% of the LC–calcine surface area resides in the pores smaller than 50 Å. In spite of the relatively high surface area to volume ratio this pore structure offers, pore filling and pore-mouth plugging occur predominantly in these small pores. In the event of pore-mouth plugging, further SO_2 access into the inner pore region is severely limited, and the sulfation rapidly dies off (Simons and Garman, 1986; Milne and Pershing, 1987).

Analysis of the sorbent properties for maximizing 50 – 200 Å pores

Assume $CaCO_3$ with a total pore volume of V_0 (cc/gmol) calcines completely to CaO. Let f_v be the fraction of the total pore volume in a specific size range, with r_f being the average pore radius, and l_f being the total pore length used to represent the pore volume, V_f ($= f_v * V_0$) in that pore-size

range. Assuming no change in the pore length and no effect of sintering, the void volume balance for the given pore-size range can be written as

$$\pi(r_f + \Delta r)^2 l_f - \pi r_f^2 l_f = v_s - v_c. \tag{17}$$

Since V_f can be expressed as

$$V_f = f_v V_0 = \pi r_f^2 l_f, \tag{18}$$

Eq. 17 can be rewritten to express the change in pore radius, Δr:

$$\Delta r = r_f \left[\sqrt{1 + \frac{(v_s - v_c)}{f_v V_0}} - 1 \right]. \tag{19}$$

The preceding analysis represents the increase in the average pore radius of a specific pore-size range. For a given V_0, Δr increases with decreasing f_v, as seen in Figure 16. Since maximization of the pores in the 50–200 Å in the calcine formed is desired, the preceding analysis can be used to provide guidelines for the sorbent pore distribution characteristics. Consider two original sorbents of identical pore volumes, V_0, but having different fractions of their total pore volume in the 50–200 Å size range. The sorbent with higher f_v would show lower Δr, thus retaining more of the pores in the 50–200 Å size range. On the other hand, for the pores in the < 50 Å range in the original sorbent, a low f_v would shift these small pores into the higher size range. Thus, a large fraction of pores in the 50–200 Å and a small fraction of pores in the < 50 Å pore sizes would represent optimum pore distribution for a sorbent.

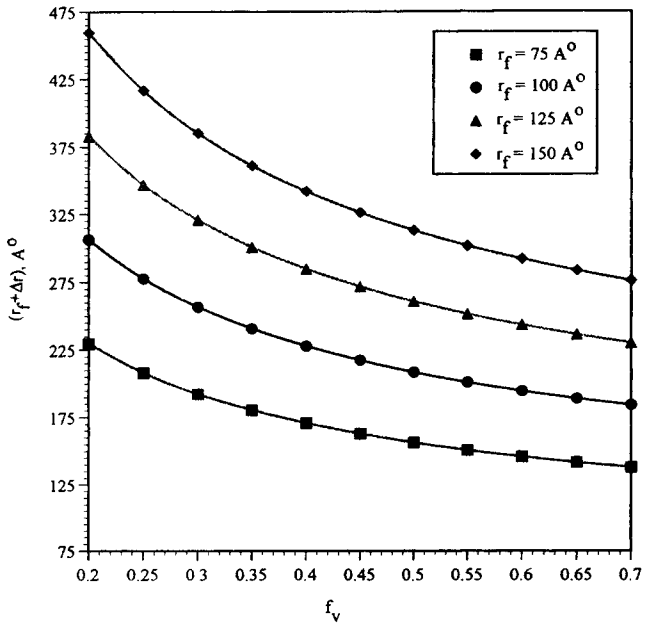

Figure 16. Increase in pore radius upon calcination as a function of the average pore radius.

$V_0 = 12$ cm³/mol.

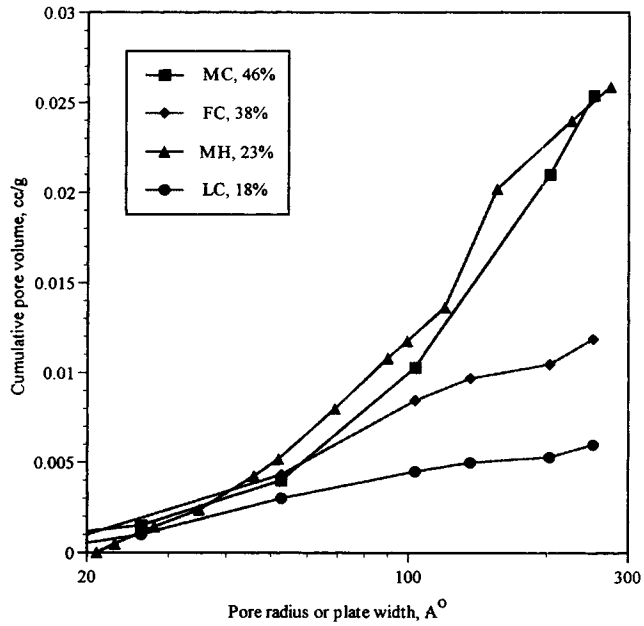

Figure 17. Pore-volume distribution after 34 ms of sulfation at 1,080°C.

Particle size: 3.9 μm.

Effect of sulfation on pore volume distribution

Figure 17 shows the pore-volume distribution after 34 ms of sulfation at 1,080°C to perform a comparative analysis between different sorbents. The sulfation extents for MC, FC, LC, and MH are 46, 38, 18, and 23, respectively. All the sorbents show a drastic reduction in total pore volume as well as the contribution of the < 50-Å pores. The MC shows the highest consumption of pore volume due to its highest conversion. The sulfation conversion curves shown in Figure 6 indicate that beyond the initial 34 ms of reaction, MC, FC, and MH show about 26%, 12%, and 15% additional conversions in the maximum allowed reaction time of about 550 ms, while only about 6 to 7% further utilization is observed in the case of LC. Figure 17 shows that the residual pore volume available for subsequent reaction is the least for LC–CaO and furthermore, most of it resides in less than 50 Å pores.

Conclusions

Most of the previous work in improving calcium-based sorbents has maximized the surface area of the parent sorbent in order to produce a high surface area and high reactivity CaO. However, such modifications failed to overcome the blockage and plugging of internal pores that lead to premature termination of sulfation. In order to maximize the sulfation capacity of calcium-based sorbents, it is established that the pores of their calcines have to lie predominantly in the 50–200 Å sizes.

In this work, the internal pore properties (surface area and pore-size distribution) of calcium carbonate sorbent are modified to improve its SO_2 reactivity. The modified carbonate exhibits exceptionally high conversion of 70–75%, which represents a nearly threefold enhancement over the commercial carbonates and hydrates. The high initial surface area and

the open pore structure of the modified carbonate translates into an optimum pore-size distribution in its calcine, which combined with the effect of slower sintering contribute to its remarkable sulfation capacity. The surface area and the pore volume in the 50–200 Å range of its calcine are maximized, which distinguishes the modified carbonate from other sorbents. Comparative investigation with other carbonates reveals that in spite of the high surface area of their calcines, the pore-size distribution shows a preferential dominance of very small pores, which leads to pore plugging and premature termination of sulfation. A modified hydrate of high surface area and porosity comparable to the modified carbonate is also investigated. The ultimate conversion as well as the initial reaction rate of the modified carbonate are nearly twice as high compared to the modified hydrate.

The results of this study illustrate the impact of internal pore structure on initial reactivity and ultimate sulfation conversion of calcium-based sorbents. It also demonstrates the potential of "tailoring" the internal pore structure of sorbents to increase their effectiveness.

Acknowledgment

This research was supported in part by the Ohio Coal Development Office. The authors would like to thank Ms. Urmila Sengupta and Mr. Himanshu Gupta for their help with the surface area and pore-size analysis.

Notation

C_s = concentration of SO_2 in bulk phase
D_p = product layer diffusivity
k_d = apparent rate constant for sulfation reaction
L_0 = total length of pore system per unit volume of calcine
P_0 = saturation vapor pressure of adsorbate nitrogen
P = vapor pressure in equilibrium with adsorbate condensed in pore
R = universal gas constant
S_0 = pore surface area per unit volume of calcine
S_g = pore surface area per unit weight of calcine
T = temperature
V_L = molar volume of adsorbate nitrogen
w_s = fraction of unreacted sorbent in partially calcined sorbent
W_p = fraction of product $CaSO_4$ in partially calcined sorbent
W_C = fraction of unsulfated CaO in partially calcined sorbent
X_c = extent of calcination of sorbent
z = ratio of molar volume of $CaSO_4$ to molar volume of CaO
ϵ = porosity of calcined, sintered, and partially sulfated CaO
ρ = molar density of CaO
γ = surface tension of adsorbate nitrogen
ν_c = molar volume of CaO
ν_s = molar volume of sorbent/$CaCO_3$

Literature Cited

Alvfors, P., and G. Svedberg, "Modeling of the Simultaneous Calcination, Sintering and Sulphation of Limestone and Dolomite," *Chem. Eng. Sci.*, **47**(8), 1903 (1992).

Bhatia, S. K., and D. D. Perlmutter, "A Random Pore Model for Fluid-Solid Reactions: II. Diffusion and Transport Effects," *AIChE J.*, **27**(2), 247 (1981a).

Bhatia, S. K., and D. D. Perlmutter, "The Effect of Pore Structure on Fluid-Solid Reactions: Application to the SO_2-Lime Reaction," *AIChE J.*, **27**(2), 226 (1981b).

Borgwardt, R. H., K. R. Bruce, and J. Blake, "An Investigation of Product-Layer Diffusivity for CaO Sulfation," *Ind. Eng. Chem. Res.*, **26**, 1993 (1987).

Borgwardt, R. H., and K. R. Bruce, "Effect of Specific Surface Area on the Reactivity of CaO with SO_2," *AIChE J.*, **32**(2), 239 (1986).

Borgwardt, R. H., "Sintering of Nascent Calcium Oxide," *Chem. Eng. Sci.*, **44**(1), 53 (1989).

Bruce, K. R., B. K. Gullett, and L. O. Beach, "Comparative SO_2 Reactivity of CaO Derived from $CaCO_3$ and $Ca(OH)_2$," *AIChE J.*, **35**(1), 37 (1987).

Cole, J. A., J. C. Kramlich, G. S. Samuelsen, W. R. Seeker, and G. D. Silcox, "Reactivity of Calcium-Based Sorbents for SO_2 Control," *Proc. First Joint Symp. on Dry SO_2 and Simultaneous SO_2/NO_x Control Technol.*, Vol. 1, EPA-600/9-85-020a (NTIS PB85-232553) (1985).

Cole, J. A., J. C. Kramlich, W. R. Seeker, G. D. Silcox, G. H. Newton, D. J. Harrison, and D. W. Pershing, "Fundamental Studies on Sorbent Reactivity in Isothermal Reactors," *Proc. First Joint Symp. on Dry SO_2 and Simultaneous SO_2/NO_x Control Technol.*, Vol. 1, EPA-600/9-86-029a (NTIS PB87-120465) (1986).

Fan, L.-S., A. Ghosh-Dastidar, and S. K. Mahuli, "Chemical Sorbent and Methods of Making and Using Same," U.S. Patent, pending (1997).

Ghosh-Dastidar, A., S. Mahuli, L. Xukun, R. Agnihotri, and L.-S. Fan, "Role of Powder Agglomeration in Ultrafast Sulfur Capture with Pure and Modified $Ca(OH)_2$," AIChE Meeting, San Francisco (1994).

Ghosh-Dastidar, A., S. Mahuli, R. Agnihotri, and L.-S. Fan, "Ultrafast Calcination and Sintering of $Ca(OH)_2$ Powder: Experimental & Modeling," *Chem. Eng. Sci.*, **50**(13), 2029 (1995).

Ghosh-Dastidar, A., S. Mahuli, R. Agnihotri, and L.-S. Fan, "Investigation of High-Reactivity Calcium Carbonate Sorbent for Enhanced SO_2 Capture," *Ind. Eng. Chem. Res.*, **35**(2), 598 (1996).

Gregg, S. J., and K. S. W. Sing, *Adsorption, Surface Area and Porosity*, Academic Press, New York, p. 111 (1982).

Gullett, B. K., and K. R. Bruce, "Pore Distribution Changes of Calcium Based Sorbents Reacting with Sulfur Dioxide," *AIChE J.*, **33**, 1719 (1987).

Gullett, B. K., J. A. Blom, and G. R. Gillis, "Design and Characterization of a 1200°C Entrained Flow, Gas/Solid Reactor," *Rev. Sci. Instrum.*, **59**(9), 1980 (1988).

Hartman, M., and O. Trnka, "Influence of Temperature on Reactivity of Limestone Particles with Sulfur Dioxide," *Chem. Eng. Sci.*, **35**, 1189 (1980).

Hsia, C., G. R. St. Pierre, K. Raghunathan, and L.-S. Fan, "Diffusion through $CaSO_4$ Formed During the Reaction of CaO with SO_2 and O_2," *AIChE J.*, **39**(4), 698 (1993).

Hsia, C., G. R. St. Pierre, and L.-S. Fan, "Isotope Study on Diffusion in $CaSO_4$ Formed during Sorbent-Flue Gas Reaction," *AIChE J.*, **41**(10), 2337 (1995).

Hu, N., and A. W. Scarone, "Fragmentation of Calcium-based Sorbents under High Heating Rate, Short Residence Time Conditions," *Fuel*, **74**(3), 374 (1995).

Innes, W. B., "Use of a Parallel Plate Model in Calculation of Pore Size Distribution," *Anal. Chem.*, **29**(7), 1069 (1957).

Kirchgessner, D. A., and W. Jozewicz, "Enhancement of Reactivity in Surfactant-modified Sorbents for Sulfur Dioxide Control," *Ind. Eng. Chem. Res.*, **28**(4), 413 (1989).

Kirchgessner, D. A., and J. M. Lorrain, "Lignosulfonate-modified Calcium Hydroxide for Sulfur Dioxide Control," *Ind. Eng. Chem. Res.*, **26**(11), 2397 (1987).

Lee, R. J., and L.-S. Fan, "The Effect of Solid Interaction Forces on Pneumatic Handling of Sorbent Powders," *AIChE J.*, **39**(6), 1018 (1993).

Mai, M. C., and T. F. Edgar, "Surface Area Evolution of Calcium Hydroxide during Calcination and Sintering," *AIChE J.*, **35**(1), 30 (1989).

Milne, C. R., and D. W. Pershing, "Time Resolved Sulfation Rate Measurements for Sized Sorbents," *Proc. Pittsburgh Coal Conf.*, p. 109 (1987).

Milne, C. R., G. D. Silcox, D. W. Pershing, and D. A. Kirchgessner, "High-temperature, Short-time Sulfation of Calcium-based Sorbents. 2. Experimental Data and Theoretical Model Predictions," *Ind. Eng. Chem. Res.*, **29**(11), 2201 (1990).

Newton, G. H., S. L. Chen, and J. C. Kramlich, "Role of Porosity Loss in Limiting SO_2 Capture by Calcium Based Sorbents," *AIChE J.*, **35**(6), 988 (1989).

Nicholson, D., "Variation of Surface Area During the Decomposition of Solids," *Trans. Faraday Soc.*, **61**, 990 (1965).

Raghunathan, K., A. Ghosh-Dastidar, and L.-S. Fan, "A Technique for the Study of Ultrafast Gas-Solid Reactions for Residence Times less than 100 ms," *Rev. Sci. Instrum.*, **63**(11), 5469 (1992).
Raghunathan, K., A. Ghosh-Dastidar, and L.-S. Fan, "High Temperature Reactor System for Study of Ultrafast Gas-Solid Reactions," *Rev. Sci. Instrum.*, **64**(7), 1989 (1993).
Sadakata, M., T. Shinbo, A. Harano, H. Yamamoto, and H. J. Kim, "Removal of SO_2 from Flue Gas using Ultrafine CaO Particles," *J. Chem. Eng. Japan*, **24**(3), 550 (1994).
Silcox, G. D., J. C. Kramlich, and D. W. Pershing, "A Mathematical Model for the Flash Calcination of Dispersed $CaCO_3$ and $Ca(OH)_2$ Particles," *Ind. Eng. Chem. Res.*, **28**(2), 155 (1989).
Simons, G. A., and A. R. Garman, "Small Pore Closure and the Deactivation of the Limestone Sulfation Reaction," *AIChE J.*, **32**(9), 1491 (1989).
Sotirchos, S. V., and H. C. Yu, "Mathematical Modeling of Gas-Solid Reactions with Solid Product," *Chem. Eng. Sci.*, **40**, 2039 (1985).
Steciak, J., Y. A. Levendis, and D. L. Wise, "Effectiveness of Calcium Magnesium Acetate as Dual SO_2-NO_x Emission Control Agent," *AIChE J.*, **41**(3), 712 (1995).
Wang, W., Q. Zhong, Z. Ye, and I. Bjerle, "Simultaneous Reduction of SO_2 and NO_x in an Entrained Flow Reactor," *Fuel*, **74**(2), 267 (1995).
Wei, S.-H., S. K. Mahuli, R. Agnihotri, and L.-S. Fan, "High Surface Area Calcium Carbonate: Pore Structural Properties and Sulfation Characteristics," *Ind. Eng. Chem. Res.*, **36**, 2141 (1997).
Ye, Z., W. Wang, Q. Zhong, and I. Bjerle, "High Temperature Desulfurization Using Fine Sorbent Particles under Boiler Injection Conditions," *Fuel*, **74**(5), 743 (1995).

Manuscript received Feb. 14, 1997, and revision received May 1, 1997.